Research Article | Vol. 8, No. 12 | 1 Dec 2017 | BIOMEDICAL OPTICS EXPRESS 5834
Biomedical Optics EXPRESS

Two-photon microscopy imaging of oxidative stress in human living erythrocytes

GOHAR TSAKANOVA,[1,2,*] ELINA ARAKELOVA,[1] VIOLETTA AYVAZYAN,[1] ANNA AYVAZYAN,[2] STEPAN TATIKYAN,[2] ROUBEN AROUTIOUNIAN,[1,3] YEVA DALYAN,[3] SAMVEL HAROUTIUNIAN,[3] VASILI TSAKANOV,[2] AND ARSEN ARAKELYAN[1]

[1]*Institute of Molecular Biology of National Academy of Sciences of Republic of Armenia, 7 Hasratyan str., 0014, Yerevan, Armenia*
[2]*CANDLE Synchrotron Research Institute, 31 Acharyan str., 0040, Yerevan, Armenia*
[3]*Yerevan State University, 1 Alex Manoogian str., 0025, Yerevan, Armenia*
**g_tsakanova@mb.sci.am*

Abstract: Red blood cells (RBCs) are known to be the most suitable cells to study oxidative stress, which is implicated in the etiopathology of many human diseases. The goal of the current study was to develop a new effective approach for assessing oxidative stress in human living RBCs using two-photon microscopy. To mimic oxidative stress in human living RBCs, an *in vitro* model was generated followed by two-photon microscopy imaging. The results revealed that oxidative stress is clearly visible on the two-photon microscopy images of RBCs under oxidative stress compared to no fluorescence in controls ($P<0.0001$). This novel approach for oxidative stress investigation in human living RBCs could efficiently be applied in clinical research and antioxidant compounds testing.

OCIS codes: (170.0170) Medical optics and biotechnology; (170.3880) Medical and biological imaging; (170.1530) Cell analysis; (170.2520) Fluorescence microscopy.

References and links

1. B. Halliwell and J. M. C. Gutteridge, "Cellular responses to oxidative stress: adaptation, damage, repair, senescence and death," in *Free Radicals in Biology and Medicine,* 4th ed., B. Halliwell and J. M. C. Gutteridge, eds. (New York: Oxford University Press, 2007), 187–267.
2. K. B. Pandey, N. Mishra, and S. I. Rizvi, "Protein oxidation biomarkers in plasma of type 2 diabetic patients," Clin. Biochem. **43**(4-5), 508–511 (2010).
3. K. B. Pandey, M. M. Mehdi, P. K. Maurya, and S. I. Rizvi, "Plasma protein oxidation and its correlation with antioxidant potential during human aging," Dis. Markers **29**(1), 31–36 (2010).
4. M. Bryszewska, I. B. Zavodnik, A. Niekurzak, and K. Szosland, "Oxidative processes in red blood cells from normal and diabetic individuals," Biochem. Mol. Biol. Int. **37**(2), 345–354 (1995).
5. W. G. Siems, O. Sommerburg, and T. Grune, "Erythrocyte free radical and energy metabolism," Clin. Nephrol. **53**(1 Suppl), S9–S17 (2000).
6. A. Kinoshita, Y. Nakayama, T. Kitayama, and M. Tomita, "Simulation study of methemoglobin reduction in erythrocytes. Differential contributions of two pathways to tolerance to oxidative stress," FEBS J. **274**(6), 1449–1458 (2007).
7. L. M. Al-Naama, M. K. Hassan, and J. K. Mehdi, "Association of erythrocytes antioxidant enzymes and their cofactors with markers of oxidative stress in patients with sickle cell anemia," Qatar Med. J. **2015**(2), 14 (2016).
8. F. Della Rovere, A. Granata, M. Broccio, A. Zirilli, and G. Broccio, "Hemoglobin oxidative stress in cancer," Anticancer Res. **15**(5B), 2089–2095 (1995).
9. C. E. Pinzón-Díaz, J. V. Calderón-Salinas, M. M. Rosas-Flores, G. Hernández, A. López-Betancourt, and M. A. Quintanar-Escorza, "Eryptosis and oxidative damage in hypertensive and dyslipidemic patients," Mol. Cell. Biochem. **434**, 1–9 (2017).
10. G. Tsakanova, E. Arakelova, A. Soghoyan, and V. Ayvazyan, "Oxidative stress and post-ischemic inflammatory response in ischemic stroke complicated with diabetes mellitus type 2," J. Biosci. Med. **3**, 94–98 (2015).
11. A. Boyajyan, M. Hovsepyan, E. Arakelova, and G. Tsakanova, "Neuroimmune alterations in diabetes: implications to molecular pathomechanisms of complications," in *Research on Diabetes II* (iConcept Press Ltd., USA, 2014). 281–297.
12. G. V. Tsakanova, V. A. Ayvazyan, A. S. Boyajyan, E. A. Arakelova, G. S. Grigoryan, A. A. Guevorkyan, and A. A. Mamikonyan, "Comparative analysis of the antioxidant system capacity and intensity of lipid peroxidation

#307127 https://doi.org/10.1364/BOE.8.005834
Journal © 2017 Received 22 Sep 2017; revised 5 Nov 2017; accepted 20 Nov 2017; published 30 Nov 2017

Biomedical Optics EXPRESS

process in ischemic stroke complicated and none-complicated with diabetes mellitus type 2 and in diabetes mellitus type 2," Bull. Exp. Biol. Med. **151**(5), 496–500 (2011).
13. H. Kaynar, M. Meral, H. Turhan, M. Keles, G. Celik, and F. Akcay, "Glutathione peroxidase, glutathione-S-transferase, catalase, xanthine oxidase, Cu-Zn superoxide dismutase activities, total glutathione, nitric oxide, and malondialdehyde levels in erythrocytes of patients with small cell and non-small cell lung cancer," Cancer Lett. **227**(2), 133–139 (2005).
14. R. Nowakowski, P. Luckham, and P. Winlove, "Imaging erythrocytes under physiological conditions by atomic force microscopy," Biochim. Biophys. Acta **1514**(2), 170–176 (2001).
15. H.-J. Butt, E. K. Wolff, S. A. C. Gould, B. Dixon Northern, C. M. Peterson, and P. K. Hansma, "Imaging cells with the atomic force microscope," J. Struct. Biol. **105**(1-3), 54–61 (1990).
16. S. A. C. Gould, B. Drake, C. B. Prater, A. L. Weisenhorn, S. Manne, H. G. Hansma, P. K. Hansma, J. Missie, M. Longmire, V. Elings, B. Dixon Northern, B. Mukergee, C. M. Peterson, W. Stoeckenius, T. R. Albrecht, and C. F. Quate, "From atoms to integrated circuit chips, blood cells, and bacteria with the atomic force microscope," J. Vac. Sci. Technol. A **8**, 369–373 (1990).
17. P. Prieto, M. Pineda, and M. Aguilar, "Spectrophotometric quantitation of antioxidant capacity through the formation of a phosphomolybdenum complex: specific application to the determination of vitamin E," Anal. Biochem. **269**(2), 337–341 (1999).
18. W. Brandwilliams, M. E. Cuvelier, and C. Berset, "Use of a free-radical method to evaluate antioxidant activity," Food Sci. Technol. (Campinas) **28**, 25–30 (1995).
19. W. Denk, J. H. Strickler, and W. W. Webb, "Two-photon laser scanning fluorescence microscopy," Science **248**(4951), 73–76 (1990).
20. F. Mao, Q. Xing, K. Wang, L. Lang, Zh. Wang, L. Chai, and Q. Wang, "Optical trapping of red blood cells and two-photon excitation-based photodynamic study using a femtosecond laser," Opt. Commun. **256**, 358–363 (2005).
21. K. Masamoto, H. Kawaguchi, H. Ito, and I. Kanno, "Dynamic two-photon imaging of cerebral microcirculation using fluorescently labeled red blood cells and plasma," Adv. Exp. Med. Biol. **765**, 163–168 (2013).
22. WHO Guidelines on Drawing Blood: Best Practices in Phlebotomy (Geneva: WorldHealth Organization, 2010).
23. U. Sprandel and J. L. Way, *Erythrocytes as Drug Carriers in Medicine* (Plenum Press New York, 1997), Chap. VIII.
24. J. J. Gille and H. Joenje, "Cell culture models for oxidative stress: superoxide and hydrogen peroxide versus normobaric hyperoxia," Mutat. Res. **275**(3-6), 405–414 (1992).
25. R. B. Sawant, S. K. Jathar, S. B. Rajadhyaksha, and P. T. Kadam, "Red cell hemolysis during processing and storage," Asian J. Transfus. Sci. **1**(2), 47–51 (2007).
26. E. Eruslanov and S. Kusmartsev, "Identification of ROS using oxidized DCFDA and flow-cytometry," Methods Mol. Biol. **594**, 57–72 (2010).
27. D. Wu and P. Yotnda, "Production and detection of reactive oxygen species (ROS) in cancers," J. Vis. Exp. **57**(57), 3357 (2011).
28. C. Cottet-Rousselle, X. Ronot, X. Leverve, and J.-F. Mayol, "Cytometric assessment of mitochondria using fluorescent probes," Cytometry A **79**(6), 405–425 (2011).
29. A. I. Pogue, B. M. Jones, S. Bhattacharjee, M. E. Percy, Y. Zhao, and W. J. Lukiw, "Metal-sulfate induced generation of ROS in human brain cells: detection using an isomeric mixture of 5- and 6-carboxy-2′,7′-Dichlorofluorescein Diacetate (Carboxy-DCFDA) as a cell permeant tracer," Int. J. Mol. Sci. **13**(8), 9615–9626 (2012).
30. V. M. Tsakanov, G. A. Amatuni, Z. G. Amirkhanyan, L. V. Aslyan, V. Sh. Avagyan, V. A. Danielyan, H. D. Davtyan, V. S. Dekhtiarov, K. L. Gevorgyan, N. G. Ghazaryan, B. A. Grigoryan, A. H. Grigoryan, L. S. Hakobyan, S. G. Haroutiunian, M. I. Ivanyan, V. G. Khachatryan, E. M. Laziev, P. S. Manukyan, I. N. Margaryan, T. M. Markosyan, N. V. Martirosyan, Sh. A. Mehrabyan, T. H. Mkrtchyan, L. Kh. Muradyan, G. H. Nikogosyan, V. H. Petrosyan, V. V. Sahakyan, A. A. Sargsyan, A. S. Simonyan, H. A. Toneyan, A. V. Tsakanian, T. L. Vardanyan, A. S. Vardanyan, A. S. Yeremyan, S. V. Zakaryan, and G. S. Zanyan, "AREAL test facility for advanced accelerator and radiation source concepts," Nucl. Instrum. Methods Phys. Res. A **829**, 284–290 (2016).
31. V. M. Tsakanov, R. M. Aroutiounian, G. A. Amatuni, L. R. Aloyan, L. G. Aslanyan, V. Sh. Avagyan, N. S. Babayan, V. V. Buniatyan, Y. B. Dalyan, H. D. Davtyan, M. V. Derdzyan, B. A. Grigoryan, N. E. Grigoryan, L. S. Hakobyan, S. G. Haroutyunian, V. V. Harutiunyan, K. L. Hovhannesyan, V. G. Khachatryan, N. W. Martirosyan, G. S. Melikyan, A. G. Petrosyan, V. H. Petrosyan, A. A. Sahakyan, V. V. Sahakyan, A. A. Sargsyan, A. S. Simonyan, S. Sh. Tatikyan, G. V. Tsakanova, E. Tsovyan, A. S. Vardanyan, V. V. Vardanyan, A. S. Yeremyan, H. N. Yeritsyan, and G. S. Zanyan, "AREAL low energy electron beam applications in life and materials sciences," Nucl. Instrum. Methods Phys. Res. A **829**, 248–253 (2016).
32. C. A. Schneider, W. S. Rasband, and K. W. Eliceiri, "NIH Image to ImageJ: 25 years of image analysis," Nat. Methods **9**(7), 671–675 (2012).
33. E. C. Jensen, "Quantitative analysis of histological staining and fluorescence using ImageJ," Anat. Rec. (Hoboken) **296**(3), 378–381 (2013).
34. F. Long, J. Zhou, and H. Peng, "Visualization and analysis of 3D microscopic images," PLOS Comput. Biol. **8**(6), e1002519 (2012).

Biomedical Optics EXPRESS

35. H. N. Kirkman, S. Galiano, and G. F. Gaetani, "The function of catalase-bound NADPH," J. Biol. Chem. **262**(2), 660–666 (1987).
36. H. N. Kirkman, M. Rolfo, A. M. Ferraris, and G. F. Gaetani, "Mechanisms of protection of catalase by NADPH. Kinetics and stoichiometry," J. Biol. Chem. **274**(20), 13908–13914 (1999).
37. G. R. Schonbaum and B. Chance, "Catalase" in *The Enzymes*, P. D. Boyer, ed., 368–408 (Academic Press, New York, 13, 1976).
38. Y. Aksoy, M. Balk, H. Ögüs, and N. Özer, "The mechanism of inhibition of human erythrocyte catalase by azide," Turk. J. Biol. **28**, 65–70 (2004).
39. F. Lang, K. S. Lang, P. A. Lang, S. M. Huber, and T. Wieder, "Mechanisms and significance of eryptosis," Antioxid. Redox Signal. **8**(7-8), 1183–1192 (2006).
40. C. Pfafferott, H. J. Meiselman, and P. Hochstein, "The effect of malonyldialdehyde on erythrocyte deformability," Blood **59**(1), 12–15 (1982).
41. G. Damonte, L. Guida, A. Sdraffa, U. Benatti, E. Melloni, G. Forteleoni, T. Meloni, E. Carafoli, and A. De Flora, "Mechanisms of perturbation of erythrocyte calcium homeostasis in favism," Cell Calcium **13**(10), 649–658 (1992).
42. T. J. Guzik, R. Korbut, and T. Adamek-Guzik, "Nitric oxide and superoxide in inflammation and immune regulation," J. Physiol. Pharmacol. **54**(4), 469–487 (2003).
43. A. Perl, P. Gergely, Jr., and K. Banki, "Mitochondrial dysfunction in T cells of patients with systemic lupus erythematosus," Int. Rev. Immunol. **23**(3-4), 293–313 (2004).
44. K. Rahman, "Studies on free radicals, antioxidants, and co-factors," Clin. Interv. Aging **2**(2), 219–236 (2007).
45. S. I. Dikalov and D. G. Harrison, "Methods for detection of mitochondrial and cellular reactive oxygen species," Antioxid. Redox Signal. **20**(2), 372–382 (2014).
46. M. Saxena and S. Sarkar, "Fluorescence imaging of human erythrocytes by carbon nanoparticles isolated from food stuff and their fluorescence enhancement by blood plasma," Mater. Express **3**, 201–209 (2013).
47. Y. Niihara, J. Ge, O. Shalev, H. Wu, A. Tu, and K. R. Tanaka, "Desferrioxamine decreases NAD redox potential of intact red blood cells: evidence for desferrioxamine as an inducer of oxidant stress in red blood cells," BMC Clin. Pharmacol. **2**, 8 (2002).
48. C. T. Evelo, A. A. Spooren, R. A. Bisschops, L. G. Baars, and J. M. Neis, "Two mechanisms for toxic effects of hydroxylamines in human erythrocytes: involvement of free radicals and risk of potentiation," Blood Cells Mol. Dis. **24**(3), 280–295 (1998).
49. Y. Miura, G. Huettmann, R. Orzekowsky-Schroeder, P. Steven, M. Szaszák, N. Koop, and R. Brinkmann, "Two-photon microscopy and fluorescence lifetime imaging of retinal pigment epithelial cells under oxidative stress," Invest. Ophthalmol. Vis. Sci. **54**(5), 3366–3377 (2013).
50. C. de la Haba, J. R. Palacio, P. Martínez, and A. Morros, "Effect of oxidative stress on plasma membrane fluidity of THP-1 induced macrophages," Biochim. Biophys. Acta **1828**(2), 357–364 (2013).
51. M. E. McLellan, S. T. Kajdasz, B. T. Hyman, and B. J. Bacskai, "In vivo imaging of reactive oxygen species specifically associated with thioflavine S-positive amyloid plaques by multiphoton microscopy," J. Neurosci. **23**(6), 2212–2217 (2003).
52. H. Wang, R. Zhang, K. R. Bridle, A. Jayachandran, J. A. Thomas, W. Zhang, J. Yuan, Z. P. Xu, D. H. Crawford, X. Liang, X. Liu, and M. S. Roberts, "Two-photon dual imaging platform for in vivo monitoring cellular oxidative stress in liver injury," Sci. Rep. **7**, 45374 (2017).
53. H. Y. Ahn, K. E. Fairfull-Smith, B. J. Morrow, V. Lussini, B. Kim, M. V. Bondar, S. E. Bottle, and K. D. Belfield, "Two-photon fluorescence microscopy imaging of cellular oxidative stress using profluorescent nitroxides," J. Am. Chem. Soc. **134**(10), 4721–4730 (2012).
54. C. Stringari, A. Cinquin, O. Cinquin, M. A. Digman, P. J. Donovan, and E. Gratton, "Phasor approach to fluorescence lifetime microscopy distinguishes different metabolic states of germ cells in a live tissue," Proc. Natl. Acad. Sci. U.S.A. **108**(33), 13582–13587 (2011).
55. M. C. Skala, K. M. Riching, A. Gendron-Fitzpatrick, J. Eickhoff, K. W. Eliceiri, J. G. White, and N. Ramanujam, "In vivo multiphoton microscopy of NADH and FAD redox states, fluorescence lifetimes, and cellular morphology in precancerous epithelia," Proc. Natl. Acad. Sci. U.S.A. **104**(49), 19494–19499 (2007).
56. R. Datta, A. Alfonso-García, R. Cinco, and E. Gratton, "Fluorescence lifetime imaging of endogenous biomarker of oxidative stress," Sci. Rep. **5**, 9848 (2015).
57. S. Mendiratta, Z. C. Qu, and J. M. May, "Erythrocyte ascorbate recycling: antioxidant effects in blood," Free Radic. Biol. Med. **24**(5), 789–797 (1998).

1. Introduction

Oxidative stress plays a crucial role in the development and progression of pathological conditions in age-related human diseases, such as diabetes, cancer, cardiovascular disorders, rheumatoid arthritis, neurological diseases, ulcers, pneumonia, cataract, glaucoma and human aging [1–3]. Among all the cells in the organism, erythrocytes or red blood cells (RBCs) are one of the first cells affected by being continuously exposed to endogenous and exogenous sources of reactive oxygen species (ROS) [4, 5]. On the other hand, the powerful antioxidant capacity of the whole blood provided by non-enzymatic and enzymatic antioxidants is

Biomedical Optics EXPRESS

contained predominantly in circulating RBCs, which allows them to maintain the oxidant/antioxidant balance in the organism [6]. However, different pathological conditions may not only trigger uncontrolled ROS generation but also lead to the alterations in the RBCs antioxidant enzyme activities and/or levels [7–9].

The above-mentioned circumstances show the benefits of studying oxidative stress in RBCs in pathological conditions. In this regard, there is a huge amount of methodologies and approaches for studying ROS in RBCs, that, however, are based on the measurement of either the end product of oxidation proteins or lipids, or the antioxidant activity of the cells, involving superoxide dismutase, catalase, glutathione, ceruloplasmin, xanthine oxidase, etc., and require the use of hemolysate of RBCs but not the cells themselves [10–13]. On the other hand, over the last years, a vast array of techniques and approaches have been developed to visualize RBCs [14–16], that however used fixed RBCs, the high resolution imaging of which was difficult to achieve due to the approximate spherical shape and high flexibility of the cells [14]. Chemical reactions that involve the generation of free radical compounds, form the basis of the most widely used methods. Mechanistically, these methods work via a single electron transfer reaction, such as the phosphomolybdenum method [17], a hydrogen atom transfer reaction between an oxidant and a free radical, or by oxidative coupling between these two species, such as the diphenyl-2-picrylhydrazyl hydrate (DPPH•) free radical assay [18].

Presently, two-photon microscopy is a powerful research tool for studying biological function in living cells and tissues. It offers a number of advantages over conventional imaging techniques, including increased imaging depths, reduced photodamage and highly localized excitation to high-resolution photochemistry [19]. Nowadays, in terms of RBCs, two-photon microscopy was used for optical trapping of RBCs [20], spatiotemporal dynamics of RBCs in three-dimensional microvascular networks of the cerebral cortex in genetically engineered rats [21].

In this paper, the results of the novel protocol development for the assessment of the oxidative stress in human living erythrocytes using two-photon microscopy are presented. The results open up new opportunities for real-time investigations of oxidative processes in human living cells that will contribute to a deeper understanding of the role of oxidative processes in pathomechanisms of various human diseases.

2. Materials and methods

2.1. Experimental design

Freshly isolated human living RBCs were subjected to H_2O_2 exposure to mimic oxidative stress. For optimization of the oxidative stress conditions 0.05%, 0.1%, 0.2%, 0.3%, 0.4% and 0.5% final peroxide concentrations were tested by the comparison of the data obtained upon the two-photon microscopy imaging and *in vitro* hemolysis assays, and the optimal condition was used for the main experiments. Two-photon microscopy imaging was performed by using a fluorescent dye, 5(6)-carboxy-2',7'-dichlorofluorescein diacetate (carboxy-DCFDA).

2.2. Study subjects

A total of 20 healthy volunteers (mean age ± SD: 30 ± 9 years, females/ males: 10/10) from the Institute of Molecular Biology NAS RA were enrolled in this study. All subjects were healthy, active and living independently at home, reporting no serious medical disorder or treatment during the past 12 months. The selection criteria excluded the subjects with chronic inflammation and/or infectious diseases, present or past history of metabolic, cardio- and cerebrovascular (diabetes mellitus, infarction, stroke, etc.), neuropsychiatric, immune system and oncological disorders, any clinical signs and symptoms of anemia or other serious medical conditions. All subjects gave their informed consent to participate in the study, which was approved by the Ethical Committee of the Institute of Molecular Biology NAS RA *(IRB #00004079)*.

Biomedical Optics EXPRESS

2.3. Blood collection and erythrocyte isolation

Practically fasting blood samples (~2 ml each) were collected by venipuncture in EDTA containing tubes using plastic syringe and relatively wide-bore needle according to the WHO guidelines on drawing blood [22]. To isolate RBCs, immediately after blood collection the blood samples (200 µl) were washed twice in isotonic saline solution (0.9% NaCl) and once in isotonic phosphate-buffered saline (PBS; NaH2PO4·2H2O 123 mmol/l, Na2HPO4 27 mmol/l, NaCl 123 mmol/l; pH 7.4) at 2000 g at 4°C for 5 minutes. The blood components, plasma and buffy coat, were removed by aspiration after the first wash, leaving RBCs at the bottom of the centrifuge tube. After the washing procedures, a suspension of RBCs was prepared by adding PBS to the washed and aliquoted RBCs (RBC-PBS solution) to obtain 1 to 10 dilution [23].

2.4. Generation of an in vitro model of oxidative stress

The RBC-PBS suspension was used as the negative control for oxidative stress. *In vitro* oxidative stress was generated by addition of peroxide to 40 µl of RBC-PBS solution (RBC-PBS-H_2O_2). In the first step RBC-PBS-H_2O_2 with 0.05%, 0.1%, 0.2%, 0.3%, 0.4% and 0.5% final peroxide concentrations were obtained in order to find the optimal concentration of H_2O_2 causing oxidative stress in human living RBCs [24]. After the incubation at 37°C for 40 minutes, the samples were washed twice in PBS under the above described conditions.

2.5. Calculation of in vitro hemolysis of erythrocytes

To calculate the percentage of the hemolysis (%H) of the samples with intact RBCs and those exposed to oxidative stress, 100% hemolysis was obtained by adding the same amount of water. The absorption of hemoglobin was spectrophotometrically measured at 540 nm in these three samples (the supernatant of the suspension of intact RBCs in PBS, the supernatant of the suspension of RBCs exposed to oxidative stress and 100% hemolysed samples). The percentage of the hemolysis was determined by using the following equation: $\%H = A/B \times 100$, where "A" is the absorbance of the supernatant and "B" is the absorption of the same sample exposed to 100% hemolysis [25].

2.6. Imaging of oxidative stress in RBCs by two-photon laser scanning microscopy

For the detection of oxidative stress inside living cells, the intact RBC-PBS and RBC-PBS-H_2O_2 samples were treated with a ROS-sensitive membrane-permeable dye, 5(6)-carboxy-2',7'-dichlorofluorescein diacetate (carboxy-DCFDA, Sigma-Aldrich Chemie GmbH, Germany) fluorescent dye, most commonly used for detection of changes in redox state in a cell [26–28]. While not excited, carboxy-DCFDA is colorless and nonfluorescent. However, upon cleavage of two acetate groups by intracellular esterases and conversion to fluorescent fluorophore, 5-(and-6)-carboxy-2',7'-dichlorofluorescein, it emits bright green fluorescence proportional to ROS generation intensity. The key reason why carboxy-DCFDA was chosen is because of the conformational rearrangements after the cleavage inside the cell it loses the permeability and therefore remains within the cell. This feature allows using carboxy-DCFDA as an indicator that can be measured in relatively wide time window [29]. Ten µl of 100 µM carboxy-DCFDA diluted in DMSO were added to each sample with the subsequent incubation at 37°C for 30 minutes. After washing with PBS, the stained cells were resuspended in 40 µl PBS and were immediately prepared for two-photon microscopy imaging.

For two-photon microscopy imaging, a drop of this suspension (2 µl) from each sample was pipetted on the center of a grease-free clean glass microscope slide and covered by a coverslip. The slide was then transferred to the microscope. All measurements were made at room temperature (20-22°C). Uniformly distributed carboxy-DCFDA fluorescence can be

Biomedical Optics EXPRESS

detected in the cell cytoplasm only if a generation of oxidative stress, i.e. generation of ROS occurs in there. All experiments were conducted in triplicate.

2.7. Laser source

The laser source used for the two-photon scanning fluorescence microscopy is a diode-pumped Yb:KGW ultrafast oscillator ("t-pulse", Amplitude Systems, France) available at the AREAL facility [30, 31]. The laser generates a high-repetition-rate (50 MHz) train of ultrashort (240 fs) pulses of quasi-monochromatic (~5 nm bandwidth) light at 1030 nm wavelength. The output average power of the oscillator is 1.1 W (energy per pulse ~22 nJ) which is too high for safe imaging of the samples. The power of the excitation is therefore regulated using a PC-controlled power attenuation kit placed in the beam path to maintain final power of 300 mW at the sample.

The uniformity of laser pulses was continuously controlled to maintain the same excitation energy during the experiment.

2.8. Two-photon fluorescence laser scanning microscopy system

The two-photon laser scanning upright microscope (MOM- Movable Objective Microscope, Sutter Instruments, USA) with 20 × water immersion objective and numerical aperture of 1.0 and 2.0 mm working distance was used to capture microscopy images of RBCs.

Beam splitter mounted into laser beam path allows to change laser power at the surface of the samples in wide range (3-500 mW), which provides acquiring good contrast without detectable morphological changes in RBCs during the time of the experiment (30–60 min). The fluorescence of carboxy-DCFDA was detected using two-channel system with green (Full Width at Half Maximum (FWHM): 70 nm; Maximum transmission: 525 nm; Average transmission: 92%) filter and a photomultiplier (R6357; Hamamatsu Photonics Deutschland GmbH, Herrsching, Germany) with 185 – 900 nm bandwidth.

For the spatial investigation, *z*-stack image analysis of cells was performed with 30-45 cross-sections for each field of view in AVI Movie format with the z-scanning depth of 12 μm. The schematic representation of the experimental set-up and the transmission spectrum of the filter are presented in Fig. 1.

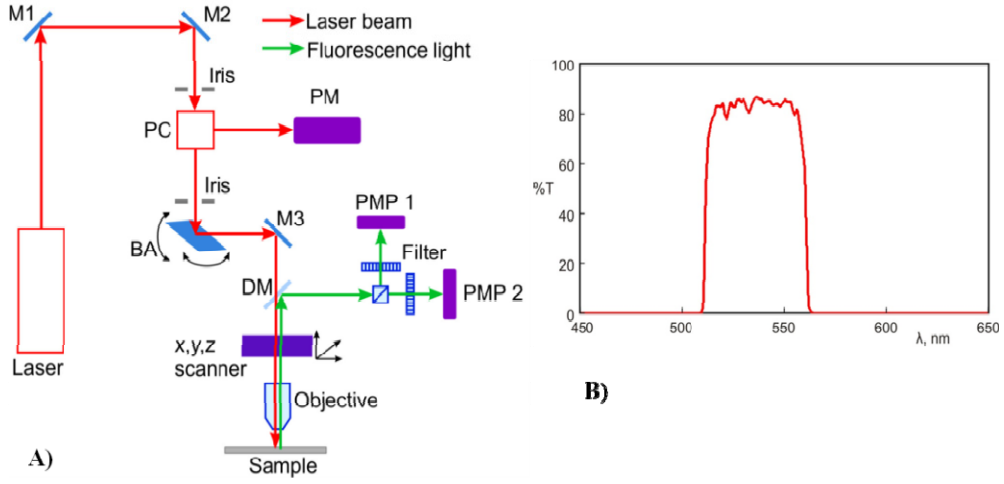

Fig. 1. A) The two-photon fluorescence laser scanning microscopy system scheme used to capture microscopy images of RBCs: M1, M2, M3 – Mirrors; PC – Polarizing cube/beam splitter; PM – Power measurement; BA – Beam adjustment mirror; DM – Dichroic mirror with cutoff wavelength of 585 nm and average transmission of 90-95%; PMP1, PMP2 – Photomultipliers; B) The transmission spectrum of the green filter used for the detection of carboxy-DCFDA fluorescence.

Biomedical Optics EXPRESS

Before two-photon excitation of the cells their transmission images in the bright field was collected using the halogen lamp illumination with blue filter. The cells within the bright field were specified as targets for subsequent two-photon laser scanning. RBCs images were obtained by x,y galvanometric scanner in standard (512x512 pixels; 3.05 fps frame rate) and high-quality (1024x1024 pixels, 0.76 fps frame rate,) modes on 12 bits photomultiplier with pixel clock of 1000 ns and magnification of 4 × . The images were false color coded for display. Image capturing and processing was conducted by the MOM microscope and ImageJ [32] software.

2.9. Image processing and data analysis

Image processing was performed using Fiji/ImageJ software (ImageJ 1.50i NIH, Bethesda, MD, USA) [32]. For the quantitative analysis of the cells fluorescence intensity in arbitrary units (AU) the acquired images were converted to 8 bit grayscale images. Afterwards, raw images were segmented by adaptive thresholding to facilitate automatic cell detection [33]. In case of merged particles the "Binary" function and "Watershed" were used. The obtained results were then analyzed using the "Particle Analyzer". By using "Freehand selections", non-detected cells were added and artificial objects were removed from the ROI. The 0-255 normalized scale was used for the selected images, where 0 corresponds to the black and 255 to the white color. The image intensity was calculated as a sum of intensities of all the cells from the ROI. Volume Viewer and 3D Viewer plugins were used for 3D deconvolution of two-photon microscopy *z*-stack images of cells [34].

Statistical analysis was performed using "Graphpad Prism 3.03" (GraphPad Software Inc., USA). The paired Student *t*-test was used to compare two conditions (with and without oxidative stress) using the original data. Groups' statistics is presented in dot plot graph. The 95% confidence interval and Pearson's value (*P*-value) were calculated to evaluate the effects of any difference. *P*-values less than 0.05 were considered statistically significant.

3. Results

3.1. Selection of the optimal oxidative stress condition in RBCs

To find the optimal H_2O_2 concentration that would cause the maximum oxidative stress to the cells and at the same time minimally affect the cell integrity, we compared the percentage of hemolysis of RBCs and the intensity of oxidative stress under different oxidative stress conditions.

In vitro hemolysis of erythrocytes. The results of the analysis of *in vitro* hemolysis of intact RBCs and those exposed to different conditions of oxidative stress with 0.05%, 0.1%, 0.2%, 0.3%, 0.4% and 0.5% H_2O_2 concentrations are presented in Fig. 2. Our data indicated the increase of peroxide induced hemolysis rate compared to intact cells in dose dependent manner. For higher H_2O_2 concentrations of 0.3%, 0.4% and 0.5%, the differences between the intact RBCs and those exposed to oxidative stress became more apparent. However, the H_2O_2 concentrations of 0.4% and 0.5% seemed to have similar releasing profile, indicating that the H_2O_2 concentration reaches a saturation level after 0.3%. This suggested that the latter is the optimal concentration to mimic oxidative stress in human living RBCs. Our data is in line with other studies, reporting that H_2O_2 concentrations more than 0.1 M inhibit the activity of catalase in human RBCs [35–38]. Moreover, these high concentrations of chemical treatment were shown to cause pronounced RBCs hemolysis which is in agreement with the known fact that chemicals harden the cell, changing the membrane deformability. In this regard, the decrease in deformability and increase in membrane stiffness in RBCs can be attributed to oxidative stress [39–41] that in our case forms intensely fluorescent localizations of ROS within the cell.

Biomedical Optics EXPRESS

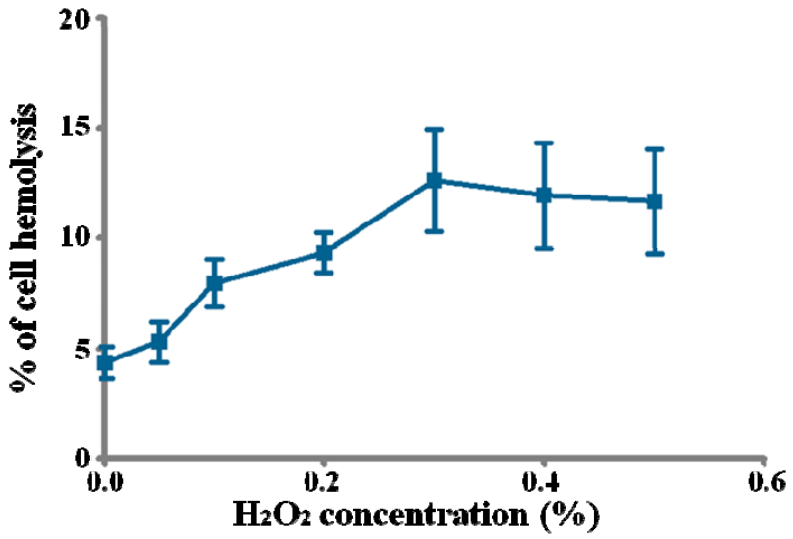

Fig. 2. The percentage of RBCs hemolysis in different conditions of oxidative stress (0.05%, 0.1%, 0.2%, 0.3%, 0.4% and 0.5%).

Two-photon fluorescence imaging of human living erythrocytes. To confirm that 0.3% is the most optimal condition for oxidative stress among the studied H_2O_2 concentrations of 0.05%, 0.1%, 0.2%, 0.3%, 0.4% and 0.5%, the suspensions were further analyzed by two-photon laser scanning fluorescence microscopy. On the two-photon microscopy images presented in Fig. 3, and the Carboxy-DCFDA fluorescence intensities obtained from the image processing and analysis of these images (Fig. 4) the same tendency of saturation level after H_2O_2 concentration 0.3% is obviously seen, which further confirmed that 0.3% concentration of H_2O_2 is the optimal condition to generate maximum oxidative stress in human living RBCs in parallel with minimal induction of cell hemolysis. Therefore, this concentration was further used in the core experiments.

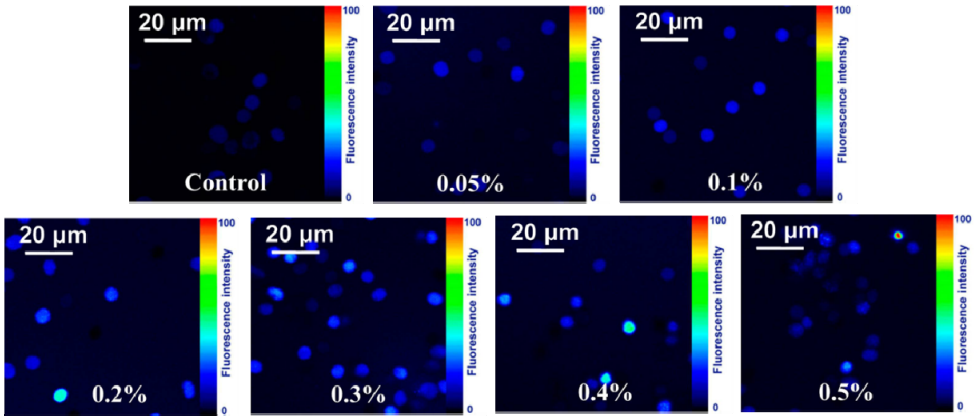

Fig. 3. Two-photon fluorescence intensity images of RBCs treated with different H_2O_2 concentrations.

Biomedical Optics EXPRESS

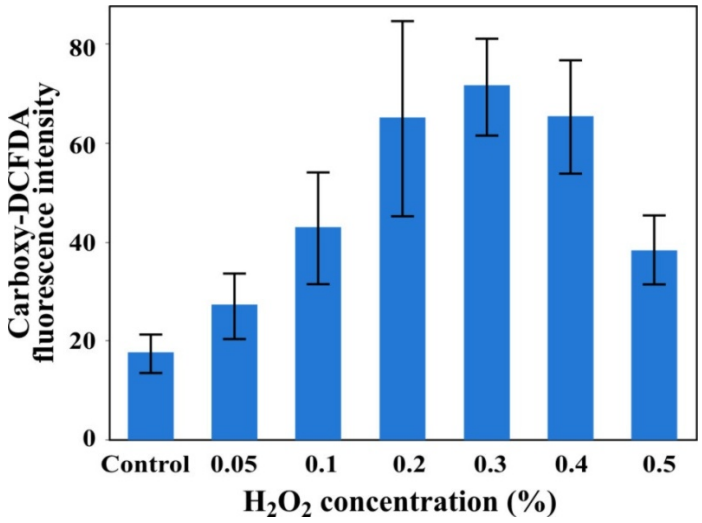

Fig. 4. Carboxy-DCFDA fluorescence intensities of the images presented in Fig. 3. Fluorescent intensities are represented in arbitrary units (AU).

3.2. The study of oxidative stress in human living erythrocytes

Prior to the main experiments, imaging of intact RBC samples was performed to ensure the presence of normal biconcave disk-shaped cells in samples. By the imaging of negative samples (without oxidative stress or H_2O_2) we ensured that we have normal RBCs with a shape of biconcave disk, but not crenated or spherical. Samples that initially demonstrated changes in the RBC morphology (crenated or spherical) were not processed further. These were 2 samples initially demonstrating crenated RBCs that were excluded (Fig. 5).

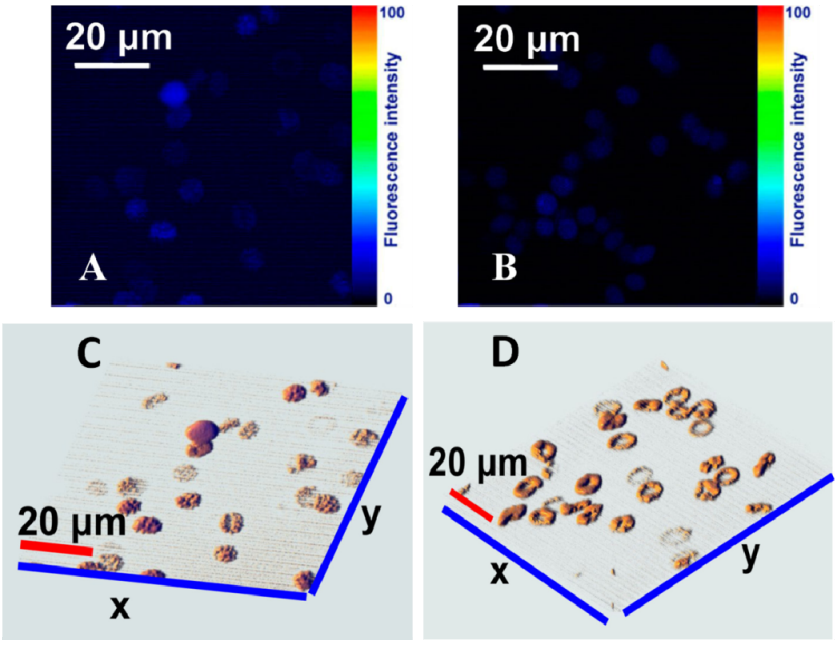

Fig. 5. (A and B) Two-photon fluorescence intensity images of initially (before the H_2O_2 exposure) crenated and excluded RBCs samples treated with carboxy-DCFDA; 3D deconvolution of two-photon microscopy *z*-stack images of crenated (C) and normal cells (D).

Biomedical Optics EXPRESS

To conduct an adequate and well-controlled study, that would exclude any possibility to register autofluorescence of the cells instead of or together with the carboxy-DCFDA fluorescence, the groups of intact RBCs and those exposed to oxidative stress were examined with the following conditions: RBCs with and without carboxy-DCFDA in bright field and RBCs with and without carboxy-DCFDA at 1030 nm. The results of the two-photon fluorescence imaging of intact RBCs and those exposed to oxidative stress are presented in Fig. 6.

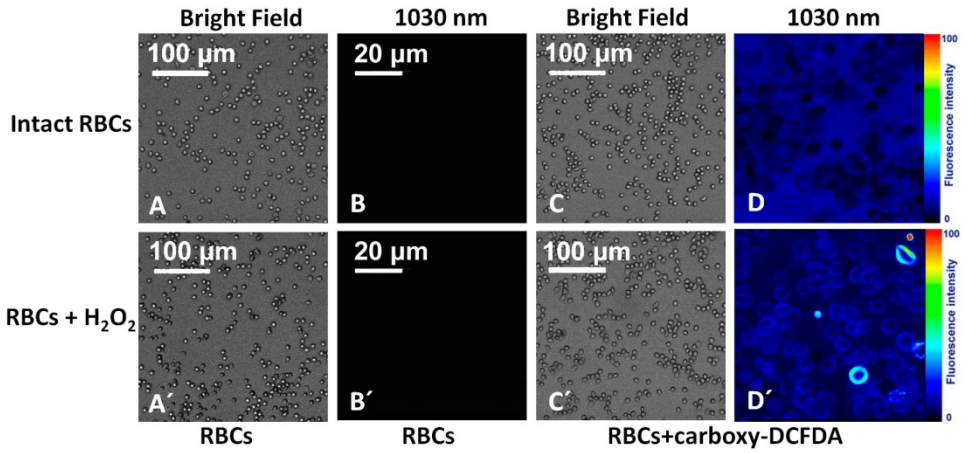

Fig. 6. Two-photon fluorescence intensity images of intact RBCs and those exposed to oxidative stress. The first row: images taken from the samples with intact RBCs (Fig. 6(A)-6(D)), the second row: samples with RBCs exposed to oxidative stress (Fig. 6(A´)-6(D´)). A and A´) RBCs without carboxy-DCFDA in bright field; B and B´) RBCs without carboxy-DCFDA in two-photon excitation; C and C´) RBCs with carboxy-DCFDA in bright field; D and D´) RBCs with carboxy-DCFDA in two-photon excitation.

The oxidative stress is clearly visible on the two-photon fluorescence microscopic image of RBCs with H_2O_2 by the carboxy-DCFDA fluorescence uniformly distributed in the cytoplasm of human living RBCs (Fig. 6(D´)), representing abundant oxidative stress processes in these cells. In contrast, no or little fluorescence was observed in controls with intact RBCs (Fig. 6(D)) (only incubation with carboxy-DCFDA), representing the absence or physiological generation of oxidative stress, respectively. Low fluorescence levels are possible due to the balanced free radical formation in normal physiological conditions. The human living RBCs (both intact and exposed to oxidative stress) neither with nor without carboxy-DCFDA do not show any fluorescence on the optical microscopic images under the excitation in bright field (Fig. 6(A), 6(A´), 6(C), 6(C´)). Further, the human living RBCs (both intact and exposed to oxidative stress) without carboxy-DCFDA do not show any fluorescence on the two-photon fluorescence microscopic images as well (Fig. 6(B), 6(B´)). Figure 6(A)-6(C) and 6(A´)-6(C´) clearly confirm that the fluorescence observed in Fig. 6(D) and 6(D´) comes definitely from carboxy-DCFDA but not from the autofluorescence signals coming from endogenous fluorophores of other intrinsic cellular compartments capable to fluorescence.

The results of the quantitative analysis of the carboxy-DCFDA fluorescence intensities for all stained samples revealed that the mean fluorescent intensities of the RBCs exposed to oxidative stress are 1.3 times significantly ($P < 0.0001$) higher than those of the RBCs without oxidative stress, thereby confirming the qualitative results (Fig. 7).

Biomedical Optics EXPRESS

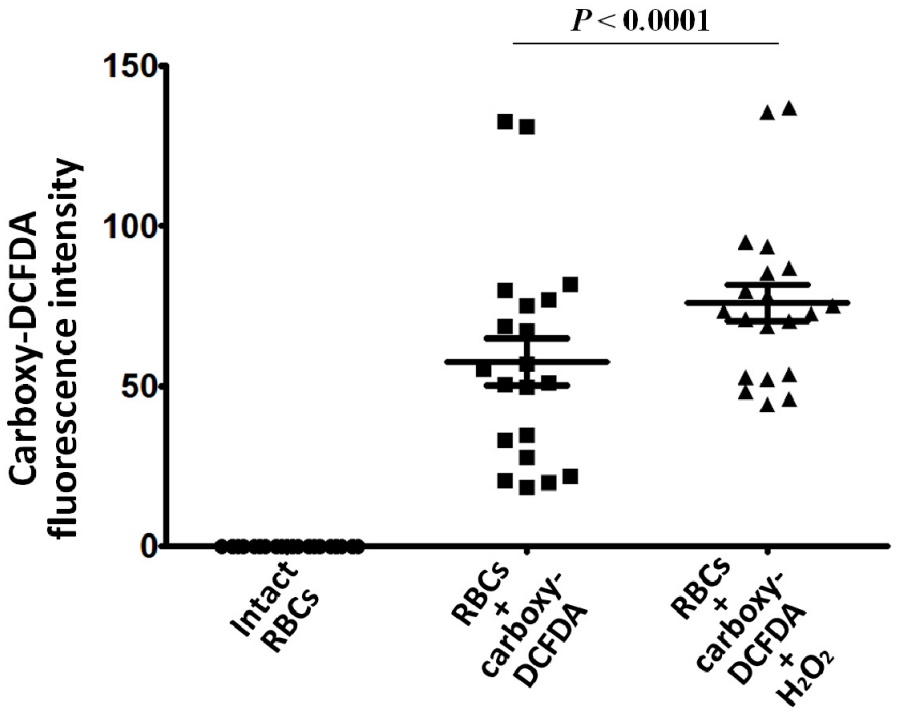

Fig. 7. The mean values of carboxy-DCFDA fluorescence intensities in samples with intact RBCs, RBCs with carboxy-DCFDA and RBCs with carboxy-DCFDA and H2O2. Each data point represents the mean intensities of single images in triplicates. Overall, 180 images were acquired (20 in each group; triplicate for each condition). In average, 30.7 ± 13.15 and 35.8 ± 14.12 (mean ± SD) cells have been counted in the ROIs for RBCs with and without H2O2.

4. Discussion

In the present paper, we described two-photon laser scanning imaging approach for the assessment of oxidative stress generated *in vitro* in human living RBCs. The RBCs freshly isolated from the blood samples of healthy volunteers were used. To mimic an oxidative stress *in vivo* event in RBCs we used hydrogen peroxide at a concentration causing oxidative stress with the minimal hemolysis of the cells. The intensity of the oxidative processes in RBCs was detected using carboxy-DCFDA membrane-permeable fluorescent dye and two-photon laser scanning microscopy technique. To our knowledge, this is the first study investigating the oxidative stress processes in living RBCs using two-photon microscopy technique. In terms of applications, the study of oxidative stress in RBCs gives an opportunity to know about the state of the antioxidant capacity of the organism. Accordingly, the proposed approach can be very important not only in the studies of the etiopathomechanisms of different diseases but also in the studies of the effects of different agents, drugs, extracts and irradiation on RBCs.

Oxidative stress has been shown to be involved in the etiopathological mechanisms of almost all pathological conditions (including inflammatory, autoimmune, cardiovascular and neurodegenerative diseases, as well as cancer, diabetes, aging) and treatment types (radiation, chemotherapy, etc.) [1–3, 42–44]. That makes the detection and measurement of ROS generation a highly interesting and important task in the investigations of the etiopathological processes of these diseased conditions in many basic, pre-clinical and clinical studies [27].

Biomedical Optics EXPRESS

ROS have very short half-lives, making these species excellent signaling molecules, but at the same time complicating their detection. Nevertheless, in last decade, numerous methods have been developed and are routinely used to evaluate ROS production [45–48], including their detection using carboxy-DCFDA [27, 49].

It should be noted that the method of two-photon microscopy also has its prominent importance among these approaches. Thus, this technique allowed de la Haba et al. [50] to evaluate oxidative stress induced changes of the distribution of membrane fluidity in different domains within the plasma membrane of macrophages using Laurdan. Moreover, multiphoton imaging provided a direct observation of amyloid-β-related oxidative stress in senile plaques in Alzheimer's models of living mice [51]. A very important field is the development of molecular probes for two-photon fluorescence intensity imaging of biomarkers of oxidative stress, such as fluorescent transition-metal complexes with different specific responsive groups for detection of glutathione (GSH), hydrogen peroxide (H_2O_2) and hypochlorous acid (HOCl) [52], two-photon pro-fluorescent nitroxides for the detection and imaging of ROS [53], as well as for detection of oxidative stress-induced bright autofluorescent appearance inside and around retinal pigment epithelial cells [49]. The non-invasive and sensitive label free methods of two-photon microscopy have beneficially been used also for the autofluorescent studies of the intrinsic signals coming from endogenous fluorophores, such as autofluorescent metabolic products collagen, retinol, retinoic acid, porphyrin, autofluorescent metabolic coenzymes, such as flavin adenine dinucleotide (FAD) and nicotinamide adenine dinucleotide (NADH) [54, 55], autofluorescence of oxidized lipids [56].

However, there is still a demand for the development of sensitive methods for detection of oxidative stress both in RBCs and in living cells. In this study, we have concentrated our efforts on RBCs, since they may be considered mobile free radical scavengers due to their ability to provide antioxidant protection not only to themselves but also to all the cells in the organism they supply with oxygen [5, 57]. Moreover, RBCs are not widely used in the investigations, because it is very hard to obtain them and keep in native state. Thus, enhanced oxidative stress can be imaged in living RBCs by two-photon laser scanning microscopy making this a potentially useful and reliable approach to track oxidative stress longitudinally in the human living RBCs. Characteristically, the intentional, prolonged exposure to 1030 nm excitation pulses for imaging over 15 minutes did not cause measurable photobleaching or photodamage to the RBCs.

The possible limitation of the application of this approach can be the necessity to use RBCs freshly isolated from blood samples. Also, there may be a need to change the optimal concentration of H_2O_2 to mimic the oxidative stress in living RBCs collected from other populations, taken into account the antioxidant system specificities between different populations.

With regard to the development prospective, experiments have to be done to obtain more detailed imaging, providing the detection of oxidative processes on subcellular levels, particularly, membrane, cytoplasm, organelle, etc. Moreover, the described approach can be used not only for the detection of oxidative stress or ROS production in different pathological conditions and oxidative stress mediated diseases, but can also be extended to other cell types and tissue samples.

5. Conclusion

In conclusion, we demonstrated a novel approach for the investigation of oxidative stress in human living RBCs that could efficiently be applied in clinical research and testing of antioxidant compounds. Moreover, it was shown that two-photon laser scanning imaging is a valuable tool for studying oxidative stress in living RBCs under oxidative stress related different pathological conditions, including diseases, inflammatory processes, aging, effects of different compounds and radiation exposure on the organism, etc.

Biomedical Optics EXPRESS

Funding

State Committee of Science MES RA (14AR-1f09, 16YR-1F011 and 17A-1F009).

Disclosures

The authors declare that there are no conflicts of interest related to this article.